

The Fourth Italian Workshop on Landslides

One-dimensional mathematical modelling of debris flow impact on open-check dams

Luca Cozzolino^{a*}, Veronica Pepe^a, Renata Della Morte^a, Vincenzo Cirillo^a, Andrea D'Aniello^b, Luigi Cimorelli^b, Carmine Covelli^b, Francesco Morlando^b, Domenico Pianese^b

^aUniversità degli Studi di Napoli Parthenope, Centro Direzionale di Napoli – Isola C4, Napoli 80142, Italy

^bUniversità degli Studi di Napoli Federico II, via Claudio 25, Napoli 80125, Italy

Abstract

The impact of debris flows on open-check dams is modeled as a Riemann problem in a rectangular cross-section channel with downstream dry state. Under the assumption that the energy is conserved through the structure, this special Riemann problem exhibits four different solution configurations. It is shown that the solution always exists, but there are ranges of the initial conditions and of the geometric characteristics for which the solution is not unique. Two different criteria for the disambiguation of the solution are proposed, and it is shown that these criteria are in agreement. The exact solutions presented can be used as internal boundary conditions in one-dimensional numerical models for the propagation of the debris-flow in river channels and narrow valleys, or as a numeric benchmark.

© 2016 The Authors. Published by Elsevier B.V. This is an open access article under the CC BY-NC-ND license (<http://creativecommons.org/licenses/by-nc-nd/4.0/>).

Peer-review under responsibility of the organizing committee of IWL 2015

Keywords: Debris-flow; Open-check dam; Impact; Riemann problem; Analytic solution; Hydraulic hysteresis.

1. Introduction

The open-check dams are frequently classified with reference to their shape and structure, or with reference to their objective and function¹. Among their objectives, it is possible to consider not only the control of the sediment discharge in mountain streams (stabilization of the longitudinal channel bed profile, consolidation of river banks,

* Corresponding author. Tel.: +39-081-5476723; fax: +39-081-5476777.
E-mail address: luca.cozzolino@uniparthenope.it

sediment retention, sorting of sediments), but also the mitigation of the debris flow propagation effects^{1,2}. During the impact of the debris flow, these structures act in several manners. First, they block large diameter boulders and driftwood (mechanical trapping function). Second, they reduce the stream width, forcing the formation of horizontal and vertical axis eddies immediately upstream, with the passage from supercritical to subcritical flow conditions (energy loss function), and this loss of energy upstream reduces the flow destructivity power. As additional effect, the deceleration of the flow induces the deposition of the small diameter sediments transported (hydraulic trapping function). Among the alternative structures, it is possible to consider slit- and sectional open-check dams. Schematically, the slit-check dams (Fig. 1a) consist of a channel constriction, where the stream width passes from b to b_0 (with $b_0 < b$) through a single opening. Conversely, sectional check-dams with fins or piles (Fig. 1b) consist of a flow obstruction where the stream width is reduced from b to b_0 through multiple openings.

Numerous experimental studies are available for these structures^{2,4}, but the numerical modeling is often required to improve the design of complex systems for the mitigation of debris flows. At the present, sophisticated two- and three-dimensional⁵ numerical models for the simulation of debris flow propagation are available. Nonetheless, these models are computationally demanding, and cheaper alternatives must be used where possible, or when the examination of numerous flow propagation scenarios is needed. In one-dimensional modeling of debris flow propagation⁶⁻⁸, which is appropriate in the case of channelized flow, the correct treatment of internal and external boundary conditions is a critical issue⁹⁻¹¹, and poor implementation of these boundary conditions may influence adversely the quality of numeric results.

In this paper, a special Riemann problem¹² is used to model the impact of debris flow on slit- and sectional check-dams, in order to supply an appropriate internal boundary condition in one-dimensional mathematical models of debris flow propagation, where the open-check dam is modelled as a width rapid transition, through which the energy is conserved^{1,2,13}. The remainder of the paper is organized as follows. First, the mathematical position of the problem is made, then the analytic solution of the special Riemann problem is supplied. Finally, it is shown that there are initial conditions for which this solution is not unique, and two different disambiguation criteria are discussed.

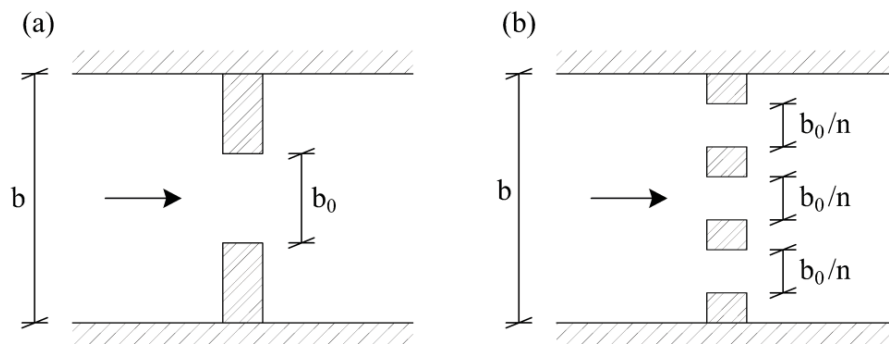


Fig. 1. Examples of open check-dams layout: (a) slit-check dam; (b) sectional check-dam with piles.

2. Analytic solution of the debris-flow impact mathematical model

In this section, the impact of the debris flow on open-check dams is modeled as the analytic solution of a special Riemann problem for the Shallow-water Equations. First, the curves used to construct the graphical solution of the Riemann problem are introduced, and then the solution is supplied.

2.1. Position of the impact model

Assuming horizontal frictionless channel with uniform rectangular cross-section, the classic Saint-Venant Equations¹⁴ can be rewritten as:

$$\frac{\partial \mathbf{u}}{\partial t} + \frac{\partial \mathbf{f}(\mathbf{u})}{\partial x} = 0, \quad (1)$$

where

$$\mathbf{u} = (h \quad hu)^T, \mathbf{f}(\mathbf{u}) = (hu \quad 0.5gh^2 + hu^2)^T. \quad (2)$$

The meaning of the symbols in Eqs (1) and (2) is as follows: x is the space coordinate; t is the time variable; h is the flow depth; u is the cross-section averaged velocity; $g = 9.81 \text{ ms}^{-2}$ is the gravitational acceleration; \mathbf{u} and $\mathbf{f}(\mathbf{u})$ are the vectors of the conserved variables and the physical fluxes, respectively, and T is the symbol of matrix transpose. Equation (1) admits two genuinely non-linear characteristic fields, and the elementary waves contained in these characteristic fields can be either rarefaction or shock waves.

The impact of the debris-flow on the open-check dam is modelled as a special initial value problem (Riemann problem¹²) where the system of Eq. (1) is solved considering the following initial conditions:

$$\mathbf{u}(x,0) = \begin{cases} \mathbf{u}_L, & x < 0 \\ \mathbf{u}_R, & x > 0 \end{cases}, \quad (3)$$

where $\mathbf{u}_L = (h_L \quad h_L u_L)^T$ is the vector of the flow characteristics of the approaching debris-flow, and $\mathbf{u}_R = (0 \quad 0)^T$ is the dry bed state. The open-check dam is located at $x = 0$, and the flow approaches the dam from the left ($u_L > 0$).

The structure of the solution for the Riemann problem of Eqs (1)–(3) is as follow: the approaching flow state \mathbf{u}_L is connected to the state \mathbf{u}_1 immediately upstream of the open-check dam by means of an elementary wave contained into the first characteristic field; the state \mathbf{u}_1 is connected to the state \mathbf{u}_2 immediately downstream of the open-check dam by means of the conditions of discharge and energy conservation; finally the state \mathbf{u}_2 is connected to the dry bed by means of a rarefaction contained into the first characteristic field.

2.2. Elementary waves and open-check dam curves

Given the generic left-hand state $\mathbf{u}_{ref} = (h_{ref} \quad h_{ref} u_{ref})^T$, the family of the right-hand states \mathbf{u} connected to \mathbf{u}_{ref} by means of an admissible shock contained in the first characteristic field is described in the (h, u) plane by the curve¹²:

$$S_1(\mathbf{u}_{ref}): \quad u = u_{ref} - (h - h_{ref}) \sqrt{0.5g(h^{-1} + h_{ref}^{-1})}. \quad (4)$$

In the same fashion, the family of the right-hand states \mathbf{u} connected to generic left-hand state \mathbf{u}_{ref} by means of an admissible rarefaction contained in the first characteristic field is described in the (h, u) plane by the curve¹²:

$$R_1(\mathbf{u}_{ref}): \quad u = u_{ref} + 2\sqrt{gh_{ref}} - 2\sqrt{gh}. \quad (5)$$

Finally, the family of the states \mathbf{u} connected to the generic state \mathbf{u}_{ref} by means of the condition of discharge per unit width conservation is an hyperbola described in the (h, u) plane by the curve:

$$CD(\mathbf{u}_{ref}): \quad u = (h_{ref} u_{ref}) / h. \quad (6)$$

If the specific energy of the flow approaching the open-check dam is greater than the energy strictly required to pass through the structure, the flow remains smooth and no transition through the critical state is expected at the

open-check dam location. On the contrary, if the energy is not sufficient, the transition through the critical state is forced. The limit condition is found imposing that the specific energy of the flow immediately upstream or downstream of the structure is equal to the specific energy of the critical flow at opening of the structure. This leads to the equation

$$h + u^2/(2g) = 1.5(b_0/b)^{-2/3} \left[(hu)^2/g \right]^{1/3}, \quad (7)$$

where b is the channel width and b_0 is the total width of the check-dam openings. The dimensionless quantity b_0/b is called *aspect ratio*. For given value of the aspect ratio, Eq. (7) admits two families of solutions of the type $u = f(h)$. In the (h, u) plane, the first family of solutions is represented by the curve

$$C_{sub} : u = K_{sub}(b_0/b) \sqrt{gh}, \quad (8)$$

where the function $K_{sub}(b_0/b)$ is defined in Eq. (18) of Appendix A. The curve C_{sub} can be interpreted as the locus of the subcritical states immediately upstream or downstream of the open-check dam, and connected to the critical state through the check dam opening. The second family of solutions is represented by the curve

$$C_{sup} : u = K_{sup}(b_0/b) \sqrt{gh}, \quad (9)$$

where the function $K_{sup}(b_0/b)$ is defined in Eq. (19) of Appendix A. The curve C_{sup} can be interpreted as the locus of the supercritical states immediately upstream or downstream of the open-check dam, and connected to the critical state through the check dam opening. If the aspect ratio tends to one, the curves C_{sub} and C_{sup} collapse onto the critical states curve C^+ defined as

$$C^+ : u = \sqrt{gh}. \quad (10)$$

In the plane (h, u) , the states above the curve C^+ are supercritical, while the states below the curve C^+ are subcritical. In the following, it will be useful to consider another limit condition, where the supercritical flow approaching the open-check dam is reverted into a subcritical flow through a standing hydraulic jump, and this subcritical flow is in turn connected to the critical state at the structure opening. Using the hydraulic jump conditions, it is easy to see that the supercritical states that satisfy this limit condition lie in the (h, u) plane on the curve defined by

$$C_{jump} : u = K_{jump}(b_0/b) \sqrt{gh}, \quad (11)$$

where the function $K_{jump}(b_0/b)$ is defined in Eq. (20) of Appendix A.

For $b_0/b < 1$ it can be demonstrated that $K_{sub}(b_0/b) < 1 < K_{sup}(b_0/b) < K_{jump}(b_0/b)$. Easy manipulations show that the limit condition of Eq. (7) can be rewritten as¹⁵

$$b_0/b = F \sqrt{27} (2 + F^2)^{3/2}, \quad (12)$$

where $F = u/\sqrt{gh}$ is the Froude number of the smooth flow immediately upstream or downstream of the open-check dam opening, and connected to the critical state flow through the open-check dam opening.

2.3. Graphical construction of the analytic solution

In the case of subcritical approaching flow ($F_L \leq 1$, where F_L is the Froude number corresponding to the state \mathbf{u}_L), two wave configurations are possible. In the first subcritical wave configuration, called SubR, the approaching flow state \mathbf{u}_L is connected to the state \mathbf{u}_1 immediately upstream of the open-check dam by means of a rarefaction. An example solution of the corresponding Riemann problem, with reference to the flow depth, is represented in Fig. 2a for $h_L = 3$ m and $u_L = 1$ m/s. The state \mathbf{u}_1 is subcritical, while the state \mathbf{u}_2 is supercritical, and this implies that critical flow conditions are attained through the width discontinuity.

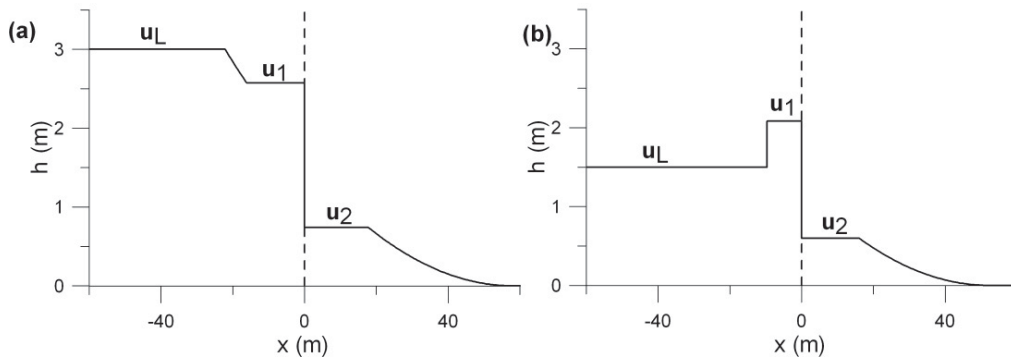


Fig. 2. Solution configurations: (a) SubR, (b) SubS.

The graphical construction of the solution in the case of the wave configuration SubR is represented in Fig. 3a. The state \mathbf{u}_1 is found at the intersection of the curves $R_1(\mathbf{u}_L)$ and C_{sub} because the state \mathbf{u}_1 is a subcritical state connected to the critical state through the width discontinuity, and it is also connected to the state \mathbf{u}_L by means of a rarefaction contained into the first characteristic field. Once that the state \mathbf{u}_1 is known, the state \mathbf{u}_2 is found at the intersection of the curves $CD(\mathbf{u}_1)$ and C_{sup} , because the state \mathbf{u}_2 has the same discharge of the state \mathbf{u}_1 and it is also a supercritical state connected to the critical state through the width discontinuity. Finally the curve $R_1(\mathbf{u}_2)$ connects the state \mathbf{u}_2 to the dry bed state.

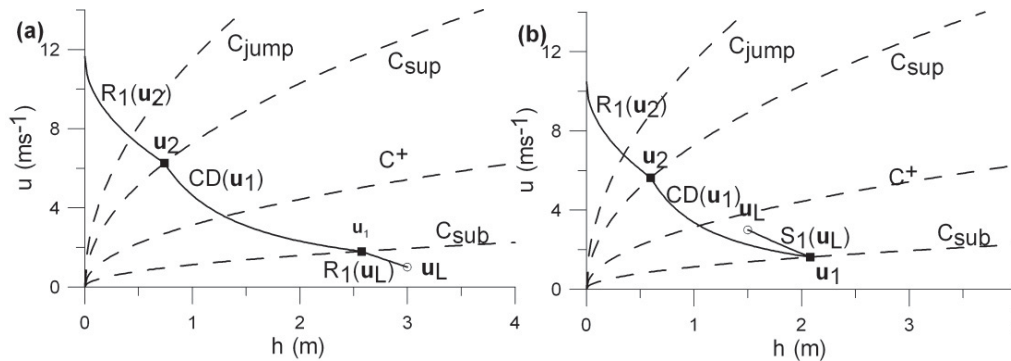


Fig. 3. Graphical construction of solutions: (a) SubR, (b) SubS.

In the second subcritical wave configuration, called SubS, the subcritical approaching flow \mathbf{u}_L is connected to the state \mathbf{u}_1 immediately upstream of the open-check dam by means of a shock. An example solution of the corresponding Riemann problem, with reference to the flow depth, is represented in Fig. 2b for $h_L = 1.5$ m and $u_L = 3$ m/s. Again, the state \mathbf{u}_1 is subcritical, the state \mathbf{u}_2 immediately downstream of the open-check dam is supercritical,

and critical flow conditions are attained through the width discontinuity. The graphical construction of the solution in the case of the wave configuration SubS is represented in Fig. 3b. The state \mathbf{u}_1 is found at the intersection of the curves $S_1(\mathbf{u}_L)$ and C_{sub} . Once that the state \mathbf{u}_1 is known, the state \mathbf{u}_2 is found at the intersection of the curves $CD(\mathbf{u}_1)$ and C_{sup} . Finally the curve $R_1(\mathbf{u}_2)$ connects the state \mathbf{u}_2 to the dry bed state.

Comparing the graphical constructions of Fig. 3, it is clear that a SubR configuration is obtained if \mathbf{u}_L lies below the curve C_{sub} , while a SubS configuration is obtained if \mathbf{u}_L lies between the curves C^+ and C_{sub} .

In the case of supercritical approaching flow ($F_L > 1$), two wave configurations are possible. In the first supercritical wave configuration, called SupNI, the approaching flow passes through the open-check dam without interacting with it because the restricted width b_0 is not sufficient to force the transition through the critical state. An example solution of the corresponding Riemann problem, with reference to the flow depth, is represented in Fig. 4a for $h_L = 0.5$ m and $u_L = 12$ m/s.

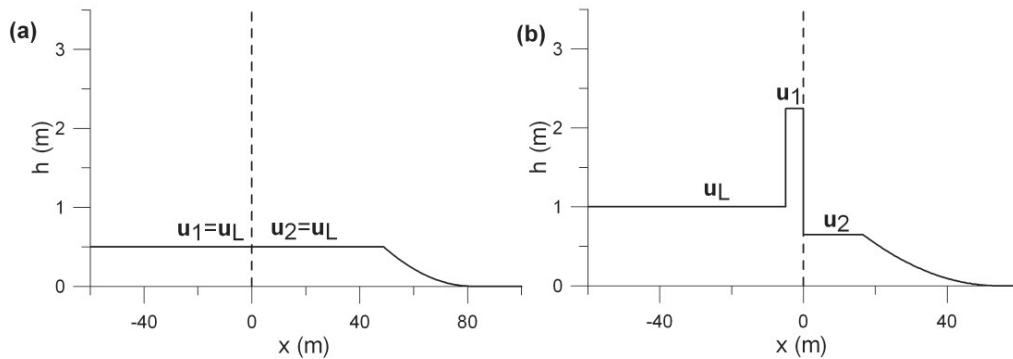


Fig. 4. Solution configurations: (a) SupNI, (b) SupS.

The graphical construction of the SupNI solution is trivial because the states \mathbf{u}_1 and \mathbf{u}_2 coincide with the state \mathbf{u}_L . The corresponding solution plot is represented in Fig. 5a.

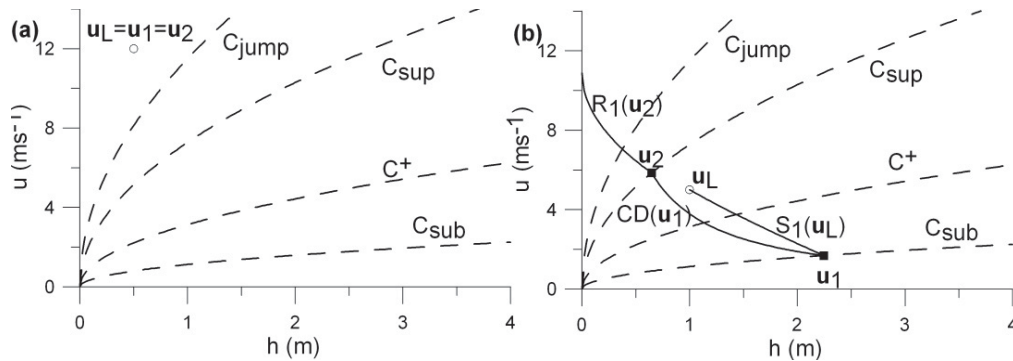


Fig. 5. Graphical construction of solutions: (a) SupNI, (b) SupS.

In the second supercritical wave configuration, called SupS, the supercritical approaching flow \mathbf{u}_L is connected to the state \mathbf{u}_1 immediately upstream of the open-check dam by means of a shock. An example solution of the corresponding Riemann problem, with reference to the flow depth, is represented in Fig. 4b for $h_L = 1$ m and $u_L = 5$ m/s. The state \mathbf{u}_1 is subcritical, the state \mathbf{u}_2 is supercritical, and critical flow conditions are attained through the width discontinuity. The corresponding graphical construction is represented in Fig. 5b, where the state \mathbf{u}_1 is found

at the intersection of the curves $S_1(\mathbf{u}_L)$ and C_{sub} . Once that the state \mathbf{u}_1 is known, the state \mathbf{u}_2 is found at the intersection of the curves $CD(\mathbf{u}_1)$ and C_{sup} . Finally the curve $R_1(\mathbf{u}_2)$ connects the state \mathbf{u}_2 to the dry bed state.

The wave configuration SupNI is admissible only if the energy of the supercritical approaching flow \mathbf{u}_L is greater than the energy strictly required to pass through the structure, and this happens only if in the plane (h, u) the state \mathbf{u}_L lies above the curve C_{sup} . By definition of the C_{jump} curve, the velocity of the shock connecting the states \mathbf{u}_L and \mathbf{u}_1 is null if the SupS solution is constructed for the states \mathbf{u}_L lying on the curve C_{jump} itself. Since the SupS wave configuration is valid only if the shock connecting the states \mathbf{u}_L and \mathbf{u}_1 has negative celerity, and moves towards upstream (see Fig. 4b), the necessary condition for having admissible SupS solutions is that \mathbf{u}_L lies between the curves C_{jump} and C^+ . From the preceding considerations, it is clear that the states \mathbf{u}_L lying between the curves C_{jump} and C_{sup} may lead to both the wave configurations SupNI and SupS.

2.4. Fields of existence

Given the graphical constructions of the Riemann problem solution, it is possible to infer the following existence conditions.

- Necessary and sufficient condition for the establishing of the solution configuration SubR is that the state \mathbf{u}_L lies below the curve C_{sub} . This is equivalent to say that

$$b_0/b \geq F_L \sqrt{27} (2 + F_L^2)^{\frac{3}{2}}, \quad F_L \leq 1. \quad (13)$$

- Necessary and sufficient condition for the establishing of the solution configuration SubS is that the state \mathbf{u}_L lies between the curves C_{sub} and C^+ . This is equivalent to say that

$$b_0/b < F_L \sqrt{27} (2 + F_L^2)^{\frac{3}{2}}, \quad F_L \leq 1. \quad (14)$$

- Necessary condition for the establishing of the solution configuration SupS is that the state \mathbf{u}_L lies between the curves C_{jump} and C^+ . This is equivalent to say that

$$b_0/b < F_L^{\#} \sqrt{27} \left[2 + (F_L^{\#})^2 \right]^{\frac{3}{2}}, \quad F_L^{\#} = F_L \sqrt{8} \left(-1 + \sqrt{1 + 8F_L^2} \right)^{-\frac{3}{2}}, \quad F_L > 1. \quad (15)$$

- Necessary condition for the establishing of the solution configuration SupNI is that the state \mathbf{u}_L lies above the curves C_{sup} . This is equivalent to say that

$$b_0/b \geq F_L \sqrt{27} (2 + F_L^2)^{\frac{3}{2}}, \quad F_L > 1. \quad (16)$$

The corresponding fields of existence are plotted in Fig 6a. The inspection of the figure shows that the union of the boundaries of the fields SubR and SupNI coincides with the limit curve obtained by Yarnell under the assumption of energy conservation¹⁵. In addition, the upper limit of the field SupS coincides with the limit of the Weak Interaction defined by Defina and Susin¹⁶. Of course, the curves presented in the cited works are studied considering steady flow regimes, while the same limits are obtained in the present work as boundaries between different wave configurations in a Riemann problem.

Interestingly, the conditions of Eqs (15) and (16) are only necessary, but not sufficient. Actually, a closer inspection of Fig. 6a shows that the fields of existence of the solution configurations SupNI and SupS are partially superposed. In other words, there is a range of supercritical initial conditions and geometric characteristics of the system for which the solution of the Riemann problem is not unique. A similar bifurcation phenomenon is discussed

in Defina and Susin¹⁶, making reference to steady flow conditions (hydraulic hysteresis). It is clear that a disambiguation criterion must be invoked in order to pick up the physically relevant wave configuration in the field where the solution of the initial value problem is not unique.

2.5. Physical disambiguation criterion

In Cozzolino et al.¹⁰ it is shown that there are initial conditions for which the Riemann problem at the non-submerged broad-crested weir is not unique, and a disambiguation criterion based on the results supplied by laboratory experiments is suggested. It is easy to recognize that this disambiguation criterion coincides with a principle of discharge maximization for given energy jump available. In addition, the dam-break at partially lifted sluice gates is considered in Cozzolino et al.¹¹, and again it is shown that there are ranges of the initial conditions for which the solution is not unique. The comparison with laboratory experiments suggests that a disambiguation criterion based on the maximization of the discharge through the device for given energy jump available is able to pick up the physically relevant solution. Based on these successful results, and considering that the principle of discharge maximization for given energy jump seems physically well grounded, the same criterion is adopted here.

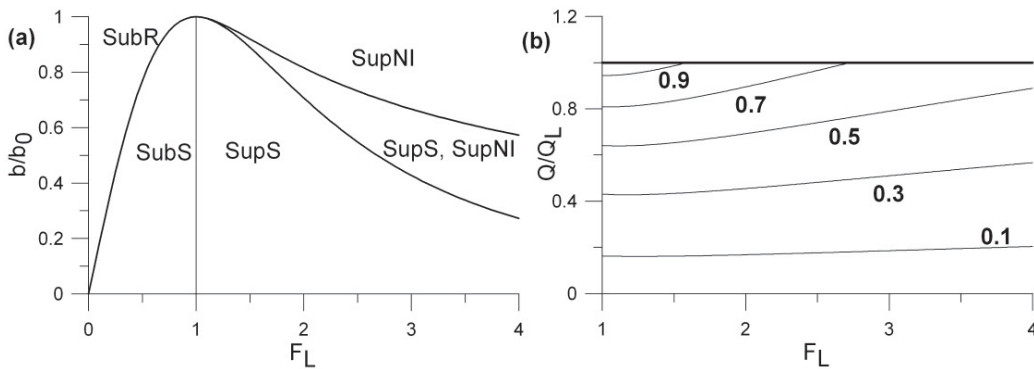


Fig. 6. Analytic solution: (a) fields of existence; (b) dimensionless discharge in the superposition field (thick black line: SupNI configuration; thin black lines: SupS configuration for different values of b_0/b)

In Fig. 6b, the ratio Q/Q_L between the discharge $Q = bh_1u_1$ through the open-check dam and the discharge $Q_L = bh_Lu_L$ associated to the approaching flow is represented as a function of the Froude number F_L . In particular, the thick black line represents the dimensionless discharge associated to the SupNI wave configuration, while the thin black lines represent the dimensionless discharge associated to the SupS configuration for different values of the aspect ratio b_0/b . It is apparent that the discharge associated to the configuration SupNI is greater than the discharge associated to the configuration SupS in the entire field where this is valid, and this suggests that the SupNI configuration should be chosen as physically relevant when an ambiguity arises.

2.6. Mathematical disambiguation criterion

It is possible to consider an alternative criterion based on a regularization argument of the Riemann problem. If the friction and bed slope terms are added to the one-dimensional Shallow-water Equations of Eq. (1), the profile of the steady monoclinal wave is obtained as the solution of the ordinary differential equation

$$\frac{dh}{dx} = S_0 - S_f \tag{17}$$

where S_0 and S_f are the bed and the friction slopes, while x is now a moving reference whose velocity is equal to the velocity u_L of the wave. The dimensionless solution of Eq. (17) is plotted in Fig. 7a with boundary condition $h = 0$ m at the toe of the steady wave profile ($x = 0$ m), considering the following resistance formulas: Manning's formula (thick line), Takahashi's formula for stony debris flow¹⁷ with constant energy coefficient k' (thick dotted line), and Takahashi's formula for stony debris flow with variable energy coefficient k' (thin line). In the plot, h_L is the normal depth corresponding to the bed slope S_0 and to the velocity u_L . The relative Froude number profile is represented in Fig. 7b, showing that it tends to infinity if the toe of the steady monoclinal wave is approached.

In the Riemann problem of Eqs (1)–(3), it is assumed that the flow depth profile of the approaching wave is discontinuous, but real-world wave profiles are more likely to behave as those of Fig. 7a. In this case, the contact between the approaching wave and the open-check dam happens in a very high Froude number regime, and the point representative of this impact falls in the field of the SupNI wave configuration in the plane of Fig. 6a. The reduction of the Froude number during the successive instants moves this representative point towards the region where both SupNI and SupS wave configurations are valid, but there is no reason to change the regime from SupNI to SupS if an additional external action is absent and the geometry of the obstacle is unchanged. Following this line of reasoning, the wave configuration SupNI must be preferred on the wave configuration SupS when both are possible.

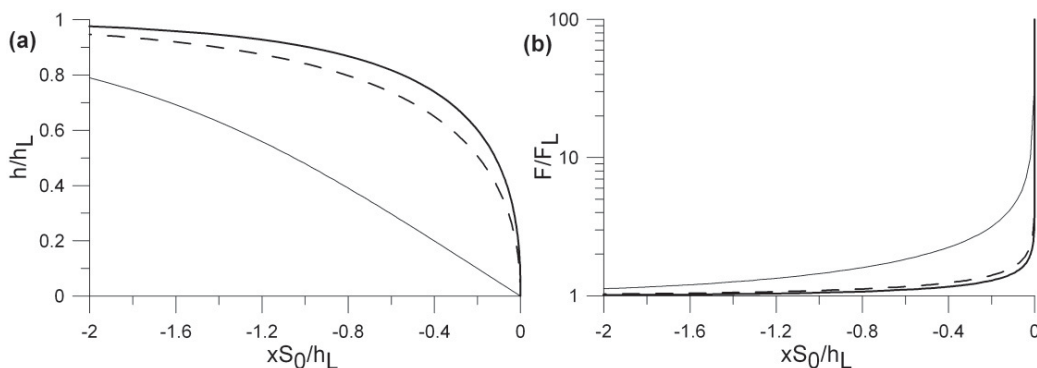


Fig. 7. Monoclonal wave: (a) dimensionless flow depth; (b) relative Froude number. Thick continuous line: Manning's formula. Thick dotted line: Takahashi's formula with k' constant. Thin line: Takahashi formula's with k' variable.

4. Conclusions

The impact of debris flows on free open-check dams in rectangular channels is modeled as a special Riemann problem where the right state is the dry bed state, while the left state coincides with a debris flow wave approaching a channel width discontinuity. In the case that the energy is conserved through the width discontinuity, this special Riemann problem exhibits four different wave configurations. It is easy to see that, independent of the initial conditions, the solution of the Riemann problem always exists, but there are cases for which the solution is not unique (bifurcation phenomenon), and two different criteria for the disambiguation of the problem solution are proposed. The first disambiguation criterion is based on physical considerations, made in analogy with other Riemann problems in open-channel flows, and it states that when two or more solutions are available, the one that maximizes the discharge must be chosen. The second disambiguation criterion is based on a purely mathematical regularization of the steady flow profile approaching the width discontinuity. Interestingly, the results supplied by these different disambiguation criteria are in agreement. The exact solutions presented can be used as internal boundary conditions in one-dimensional numerical models for the propagation of the debris-flow in mountain streams and narrow valleys, or as a benchmark for existing numeric models.

Appendix A. Definition of the coefficients in the open-check dam curves

The functions appearing in Eqs (8), (9), and (11), are defined as follows:

$$K_{sub}(b_0/b) = (b_0/b)^{-\frac{1}{2}} \left\{ 2 \cos \left[\left(5\pi - \arctan \sqrt{(b_0/b)^{-2} - 1} \right) / 3 \right] \right\}^{\frac{3}{2}} ; \quad (18)$$

$$K_{sup}(b_0/b) = (b_0/b)^{-\frac{1}{2}} \left\{ 2 \cos \left[\left(\pi - \arctan \sqrt{(b_0/b)^{-2} - 1} \right) / 3 \right] \right\}^{\frac{3}{2}} ; \quad (19)$$

$$K_{jump}(b_0/b) = k_{sub}(b_0/b) \sqrt{8} \left(-1 + \sqrt{1 + 8[k_{sub}(b_0/b)]^2} \right)^{\frac{3}{2}} . \quad (20)$$

It is easy to verify that $K_{sub}(b_0/b)$ is the solution of Eq. (12) with respect to F when the flow is subcritical, while $K_{sup}(b_0/b)$ is the solution corresponding to supercritical flow conditions.

Acknowledgement

The research was partially funded by the University of Naples Parthenope through the funding program “Sostegno alla ricerca individuale 2015-2017”.

References

1. Piton G, Recking A. Design of sediment traps with open check dams. I: Hydraulic and deposition processes. *J Hyd Engrg* 2015; 04015045.
2. Armanini A, Dalri C, Larcher M. Slit-check dams for controlling debris flow and mudflow. In: Marni H, editor. *Disaster mitigation of debris flows, slope failures and landslides*. Tokyo: Universal Academy Press; 2006. p. 141-148.
3. Armanini A, Larcher M. Ratiocal criterion for designing opening of slit-check dam. *J Hyd Engrg* 2001;127:94-104.
4. Ng CWW, Choi CE, Kwan JSH, Koo RCH, Shiu HYK, Ho KKS. Effects of baffle transverse blockage on landslide debris impedance. *Proc Earth Plan Sci* 2014;9:3-13.
5. Choi CE, Ng CWW, Law RPH, Song D, Kwan JSH, Ho KKS. Computational investigation of baffle configuration on impedance of channelized debris flow. *Can Geotech J* 2015;52:182-197.
6. Osti R, Egashira S. Method to improve the mitigative effectiveness of a series of check dams against debris flows. *Hydrol Process* 2008;22:4986-4996.
7. D’Aniello A, Cozzolino L, Cimorelli L, Covelli C, Della Morte R, Pianese D. One-dimensional simulation of debris-flow inception and propagation. *Proc Earth Plan Sci* 2014;9:112-121.
8. D’Aniello A, Cozzolino L, Cimorelli L, Della Morte R, Pianese D. A numerical model for the simulation of debris flow triggering, propagation and arrest. *Nat Haz* 2015;75:1403-1433.
9. Cimorelli L, Cozzolino L, Della Morte R, Pianese D. Analytical solutions of the linearized parabolic wave accounting for downstream boundary condition and uniform lateral inflow. *Adv Wat Res* 2014;63:57-76.
10. Cozzolino L, Cimorelli L, Covelli C, Della Morte R, Pianese D. Boundary conditions in finite volume schemes for the solution of shallow-water equations: the non-submerged broad-crested weir. *J Hydroinf* 2014;16:1235-1249.
11. Cozzolino L, Cimorelli L, Covelli C, Della Morte R, Pianese D. The analytic solution of the Shallow-water Equations with partially open sluice-gates: the dam-break problem. *Adv Wat Res* 2015;80:90-102.
12. LeVeque RJ. *Finite Volume methods for hyperbolic problems*. Cambridge: Cambridge University Press; 2004.
13. Busnelli MM, Stelling GS, Larcher M. Numerical morphological modelling of open-check dams. *J Hyd Engrg* 2001;127:105-114.
14. Barré de Saint-Venant AJC. Théorie du Mouvement Non Permanent des Eaux, avec Application aux Crues de Rivières et à l’Introduction des Marées dans leur Lit. *Compt Ren Séanc Acad Sci* 1871;73:147-154.
15. Yamell DL. *Bridge piers as channel obstructions*. Washington DC: US Department of Agriculture; 1934.
16. Defina A, Susin FM. Multiple states in open channel flow. In: Brocchini M, Trivellato F, editors. *Vorticity and turbulence effects in fluid structures interactions*. Southampton: Wessex Institute of Technology Press; 2006. p. 105-130.
17. Takahashi T. *Debris Flow. Mechanics, Prediction and Countermeasures*. Leiden: Balkema; 1991.